Enhancement of superconducting transition temperature in Nb/Pd bilayers upon rapid thermal hydrogenation

Junjie Li,[1,2,*] Ali C. Basaran,[1] Ralph El Hage,[1] and Ivan K. Schuller[1,2]

[1]*Department of Physics and Center for Advanced Nanoscience, University of California–San Diego, La Jolla, California 92093, USA*

[2]*Materials Science and Engineering Program, University of California–San Diego, La Jolla, California 92093, USA*

(Received 17 January 2023; revised 5 July 2023; accepted 16 August 2023; published xxxxxxxxxx)

Recent discoveries of high-T_c superconducting hydrides at high pressure have opened up new possibilities for improving the superconducting transition temperature (T_c) using hydrogenation. Here, a unique thermodynamic approach is developed based on the concept of rapid thermal annealing and is adopted to study the hydrogenation effect on the superconducting properties of Nb/Pd bilayer films. Below 300°C annealing temperatures, the T_c is enhanced from 8.77 to 9.06 K and is correlated with the compression of the Nb unit cell. A weak lattice expansion occurs at higher annealing temperatures, and the T_c is gradually suppressed. Furthermore, the rapid thermal hydrogenation affects the T_c differently depending on the substrate on which the Nb/Pd bilayers are grown. For the *c*-cut Al_2O_3 substrate, the T_c reduction starts at 250°C, while for the *r*-cut Al_2O_3, this occurs at 350°C. We associate these features with the elastic behavior of Nb film upon hydrogenation. A proposed model shows that the increase of T_c could be caused by the compressive stress related to the rapid nucleation of hydrides or the removal of impurities. Our discoveries provide insights into how superconductivity can be manipulated by rapid thermal hydrogenation.

DOI: 10.1103/PhysRevB.00.004500

I. INTRODUCTION

Hydrogen is the simplest, lightest, and most abundant element in the universe. Since the prediction of solid metallic hydrogen to be a high critical temperature (T_c) superconductor at ultrahigh pressure [1], searching for an alternative way of compressing hydrogen has long been an area of intensive research. Nowadays, the emphasis has moved towards compounds with high hydrogen concentration, where "chemical precompression" is believed to give rise to the metallic state at much lower pressures [2]. Several theoretical predictions have suggested that high hydrogen content in some transition metals could significantly improve the superconducting transition temperature T_c [3,4]. The rare-earth hydrides, for example, YH_{10}, were calculated to have a T_c as high as 305–326 K at 250 GPa [5], while LaH_{10} was estimated to be 274–286 K at 210 GPa [6]. However, the superconducting properties of these predictions (e.g., LaH_{10}, YH_6) have only been claimed in an ultrahigh-pressure environment, making them unsteady to obtain and even reproduce experimentally [7,8]. Moreover, it should be mentioned that earlier theoretical work [9] has also questioned the original theoretical prediction, and Eliashberg's theory might no longer be applicable in some scenarios [10]. Therefore, understanding the role of hydrogen in enhancing the T_c of superconductors experimentally is essential.

Hydrogen inclusion in known superconductors has been studied for decades [11]. It was shown that hydrogen could dissolve in niobium on tetrahedral interstitial sites, occupying specific sublattices to form a variety of hydrides that depend on temperature, pressure, and surface properties [12]. Typically, the hydrogen uptake is initially fast and slows down remarkably at relatively lower temperatures, but at higher temperatures, a rapid absorption occurs [13]. This phenomenon has been interpreted as the result of the subsurface bonding effect, where the temperature reduces the thickness of hydrogen trapping layers and enhances diffusion [14]. As a consequence, the coverage by a few monolayers of Pd on Nb could considerably improve the hydrogen uptake rate [15,16]. Moreover, a thin layer of Pd on Nb acts as a catalyst and a sieve, breaking the H_2 bond and only allowing the H atom to penetrate the Pd lattice. This prevents impurities from being incorporated in the film, which can reduce the T_c.

Nb hydrides are known to significantly suppress Nb's superconductivity, although NbH_4 is predicted, based on strong coupling Eliashberg theory, to have a T_c of 49.57 K at 300 GPa [17]. NbH and NbH_2 were found to be stable at ambient conditions but not superconducting at above 1.5 K [18]. It was shown that the T_c of NbH_x, when $x < 0.7$, remained the same or proximate to bulk niobium; at $x \geqslant 0.7$, the T_c fell suddenly below 2 K [19]. In principle, the hydrogen absorption affects the T_c of niobium mainly in three fashions: (1) A chemisorption leads to the formation of covalent bonds that share electrons from hydrogen into the common electronic band(s), increasing the valence electron density of Nb. This affects the electron-phonon coupling and, thus, the superconducting behavior [20,21]. (2) Hydrogen reduces anomalies in the acoustic phonon spectrum of Nb and may compensate for the coupling of the optical hydrogen modes, leading to a depression of T_c [11]. (3) Introducing disorders into the system decreases the T_c, resembling radiation damage or cryogenic deposition [22].

*jul018@ucsd.edu

Recently, hydrogen-induced mechanical stress as high as ∼ 8 GPa was discovered in ultrathin Nb film grown on an *a*-cut sapphire substrate [23], where a similar effect was claimed to exist in thicker films by hydrogenation. However, the superconductivity of the stressed Nb thin film upon hydrogen loading needs to be studied more in a controlled manner. Niobium hydrides were found to exist in various sizes and morphologies in thin films, ranging from small irregular shapes (5 nm) to large discrete islands (100 nm) [24]. In general, the formation of hydrides in Nb thin film can be divided into three processes: (1) Defects or impurities provide nucleation sites for hydride growth, generating a strong out of plane expansion [25]. (2) Coherent and semicoherent hydrides are formed over time, being dominant in the initial stage [26], with phase separation occurring at higher hydrogen concentrations. (3) Mechanical stress originates from the hydrides, the Nb matrix, the film, and the substrate, hindering the phase transformation. In the latter case, a maximum hydride size of ∼ 40 nm was reported in an 80 nm thick film [26].

The above findings provide us with a starting point for the development of a unique method for hydride synthesis and stress manipulation. Despite the intensive study of the Nb-H system in the past few decades, little attention was paid to understanding how the superconductivity can be controlled by a different thermodynamic approach used for hydrogenation. Previous investigations of Nb-H mainly rely on a single-step isothermal process [25–28], in which the sample is held at a constant temperature and hydrogen is applied at a constant pressure. Although this method is suitable for studying certain hydride phases, it does not provide an understanding of the evolution of niobium on a rigid substrate, which could alter the intralayer properties and affect the T_c.

Rapid thermal annealing (RTA) is a process used in semiconductor manufacturing, where it was developed to overcome the "transient-enhanced diffusion" phenomenon in silicon [29]. A typical RTA consists of a stabilization step at constant temperature, a "spike" annealing at a constant rate of ∼ 100°C/s, and cooling at ∼ 40°C/s [30]. Here, we borrowed this concept and modified RTA to make it applicable for hydrogenation: (1) We use a burst of hydrogen pressure synchronized with spike annealing, which allows the sample to enter rapidly into a thermodynamic equilibrium state (Fig. 1). (2) We apply quenching immediately after spike annealing in a hydrogen environment, which retains stress and reduces crystal grain size (Fig. 1). (3) We also eliminated the stabilization step to minimize the possibility of incorporating impurities during the process.

In the present work, an alternative thermodynamic approach was developed to create stable, T_c-enhanced superconductors at room pressure. A thin layer of Pd was deposited on Nb to induce hydrogen absorption and prevent oxidation [27]. The structural and superconducting properties are compared for the same samples before and after hydrogenation. Using the rapid thermal hydrogenation (RTH) method, the T_c of Nb/Pd bilayer films is successfully increased by ∼ 3.2% compared to its pristine state. Interestingly, lattice compression occurs whenever the T_c is enhanced, suggesting that hydrogen-induced compressive stress could be responsible for the enhancement of T_c, which is supported by the stress calculated from x-ray diffraction. A model is proposed to explain the mechanism for the effects on the T_c based on hydride nucleation and growth kinetics.

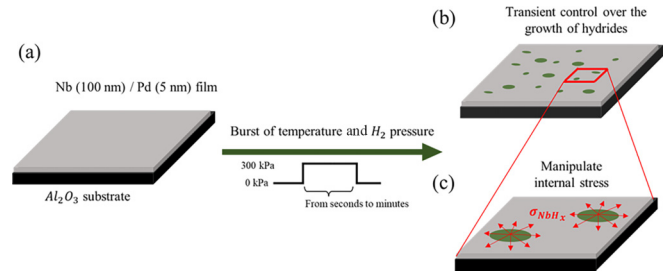

FIG. 1. Schematic illustration of the rapid thermal hydrogenation method used in this research. (a) The as-grown sample undergoes a rapid increase of temperature and hydrogen pressure, referred to as the RTH process. (b) The RTH process enables a transient control over the growth of hydrides so that the hydrogen-induced stress can be manipulated. (c) The stress presumably originates from the nucleation and growth of hydrides that may lead to the local volume changes.

II. EXPERIMENT

Nb thin films were deposited on *c*-cut and *r*-cut Al_2O_3 single crystal substrates using an *e*-beam evaporation system with a base pressure of 6.6×10^{-6} Pa. The substrates were cleaned in an ultrasonic bath with acetone, isopropanol, and methanol for 15 min at room temperature to remove impurities, and subsequently dried with compressed nitrogen gas to remove solvent residues. The *c*-cut and *r*-cut substrates were then attached to the symmetrical position of the sample holder, and the growth was done simultaneously on all substrates in the same deposition to minimize growth-related changes between different depositions. During deposition, the substrates were kept at room temperature with a deposition pressure of $\sim8.0\times10^{-6}$ Pa. Deposition rates of ∼ 0.11 and ∼0.1 nm/s were used for Nb and Pd, respectively. Film thicknesses were monitored continuously using a calibrated quartz crystal microbalance, and 100 nm of Nb with an additional 5 nm of Pd capping layer was deposited. The sample holder was constantly rotated during the deposition to ensure uniform films. To avoid sample to sample microstructural changes, the as-grown samples were cut into 4 mm×4 mm pieces and used for each hydrogenation condition.

The RTH treatment was done in a homemade rapid thermal annealing system, which is analogous to the gas evolution system previously reported [31], and its underlying concept is explained in Fig. 1. The RTH chamber consists of a thickened quartz tube and vacuum flanges that are connected by a fit-through. Experimentally, the quartz tube was preheated to the hydrogenation temperature, and kept at ∼ 10^{-5} Pa base pressure. An ultrahigh vacuum transfer arm was used to rapidly insert the sample into the quartz tube. Once the sample was loaded and the arm was retracted, the ultrahigh pure (>99.999%) hydrogen gas was then injected into the tube at a rate of ∼ 0.08 MPa/s and held at 0.3 MPa. After 30 min of hydrogenation, the tube was depressurized at a rate

of ~ 0.08 MPa/s and pumped down to high vacuum. Meanwhile, the sample was extracted using the same transfer arm, which was capable of cooling down the sample at a maximum rate of $\sim 60°$C/s. The sample was settled for at least 5 min in high vacuum before exposing to air.

The vacuum annealing was done using the same system without introducing the hydrogen gas. During the annealing, the residual gas analyzer continuously monitored the hydrogen partial pressure. The base pressure was maintained at $\sim 10^{-5}$ Pa, and hydrogen partial pressure was ensured to be better than 10^{-6} Pa.

X-ray diffraction was conducted using a Rigaku SmartLab diffractometer with Cu $K_{\alpha 1}$ radiation ($\lambda = 0.154$ nm) and a Ge-220×2 monochromator with a parallel beam configuration (PB). Thickness, roughness, and density values were obtained from x-ray reflectivity fitting using the GENX 3.6 software package [32].

Magnetization measurements were carried out using a Quantum Design DynaCool system equipped with a maximum field of 9 T and a temperature range from 1.8 to 400 K. The zero field cooling–field cooling (ZFC-FC) procedure was applied to measure the superconducting Meissner effect using the following procedure: The samples were cooled to 2 K without an applied magnetic field. The magnetization was measured in a small field of 15 Oe while warming the sample to 15 K at a rate of 2 K/min. Subsequently, the field cooling branch was measured with the same small field by cooling the sample to 2 K at the same rate. Hysteresis loops were recorded starting at zero fields for specific temperatures, and the magnetization was measured as a function of the field range from –3 to 3 T. The resistance as a function of temperature was measured using electrical transport at different magnetic fields: 0, 0.5, 1, 2.5, and 4 T. In between all measurements, the magnet was oscillated around 0 Oe to minimize residual magnetic fields, which typically were less than 4 Oe.

III. RESULTS

Figure 2 shows both the specular (a) and off-specular (b) x-ray diffraction spectra of a Nb/Pd sample grown on the c-cut sapphire substrate before and after the RTH process at 200°C. The 200°C sample is chosen because this is the maximum temperature that would enhance the superconductivity. The Nb film grown on a c-cut sapphire substrate exhibits strong (110) texture in the specular geometry as has been previously reported in the literature [33,34]. The Nb (101), (200), (211), and (310) peaks can be clearly identified from the scan and correspond to chi angles of 60°, 45°, 30°, and 26.56°, respectively. Note that the sapphire substrate peak provides an intrinsic check on the alignment and confirms that the structural changes observed are real and not due to experimental errors.

In bulk, without an anisotropic strain, the Nb (101) peak should be at the same angle as the Nb (110) peak which is reported to be at 38.61° [35]. Before hydrogenation (Fig. 2, black), in our thin film samples, the Nb (101) peak is at $\sim 38.35°$ which is $\sim 0.76°$ less than the Nb (110) peak at $\sim 39.11°$. Since the Nb (101) plane is at 60° with respect to Nb (110) plane, the Poisson's ratio of the thin film sample

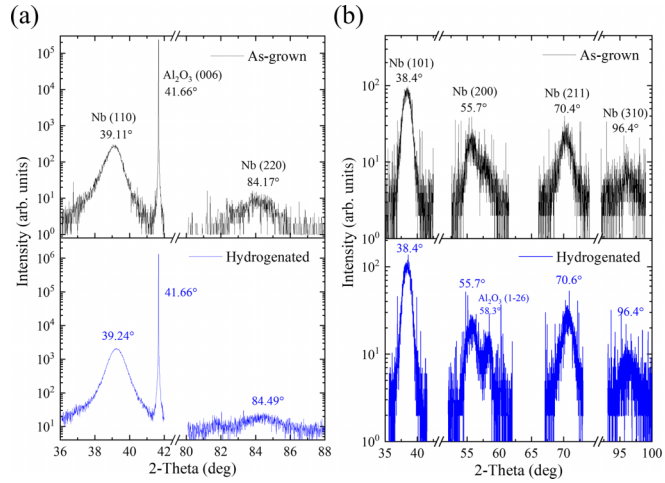

FIG. 2. X-ray diffraction of the Nb/Pd bilayer grown on c-cut sapphire substrate before and after RTH process at 200°C. (a) Specular peaks. (b) Off specular peaks. For the Nb (101) and (200) peaks, the 2-theta values are extracted from the reciprocal space maps shown in Supplemental Fig. S1 [39].

(υ_{AG}) can be estimated as follows [36]:

$$\upsilon_{AG} = -\frac{d\varepsilon_{trans}\sin\chi}{d\varepsilon_{axial}} = -\frac{(38.61° - 38.4°)\sin 60°}{38.61° - 39.1°} \approx 0.37, \quad (1)$$

where the $d\varepsilon_{trans}$ and $d\varepsilon_{axial}$ are strains in the lateral and longitudinal direction, respectively. The estimated Poisson's ratio in our sample is close to that reported in the bulk Nb ($\upsilon_{bulk} = 0.38-0.4$) [37].

The film lattice parameters extracted from the Nb (110) and Nb (220) out of plane peaks are within experimental error (0.3253 and 0.3249 nm, respectively). This implies a $\sim 1.4\%$ contraction compared to the reported bulk lattice parameter of 0.3298 nm [35]. Assuming no plastic deformation within the film, according to the linear elastic theory [23], the out of plane intrinsic stress of the thin film sample ($\sigma_{[111],\,AG}$) can be calculated by

$$\sigma_{[111],AG} = \varepsilon_{[111]}k_{[111]} = \frac{d_{(110,AG)} - d_{(110,\,lit)}}{d_{(110,\,lit)}}(154.5\ \text{GPa}), \quad (2)$$

where the $\sigma_{[111],AG}$ is positive for expansion and negative for compressive stress; $k_{[111]}$ and $\varepsilon_{[111]}$ are the stiffness [38] and the strain along the Nb [111] film direction, respectively. $d_{(110,\,AG)}$ represents the interplanar spacing of Nb (110) in the as-grown sample, and $d_{(110,lit)}$ is the interplanar spacing in a bulk Nb lattice which is equal to 0.233 nm [35]. Therefore, the as-grown c-cut sample is estimated to have an intrinsic compressive stress of ~ 7.3 GPa.

After hydrogenation (Fig. 2, blue), the Nb (110) and (220) peak positions increase and the calculated 0.3243 and 0.3239 nm lattice parameters are about 0.3% less than the as-grown sample. Based on Eq. (2), the lateral mechanical stress induced by rapid thermal hydrogenation in the same piece of sample can be calculated as follows:

$$\sigma_{[111]} = \frac{d_{(110,AH)} - d_{(110,\,BH)}}{d_{(110,\,BH)}}(154.5\ \text{GPa}), \quad (3)$$

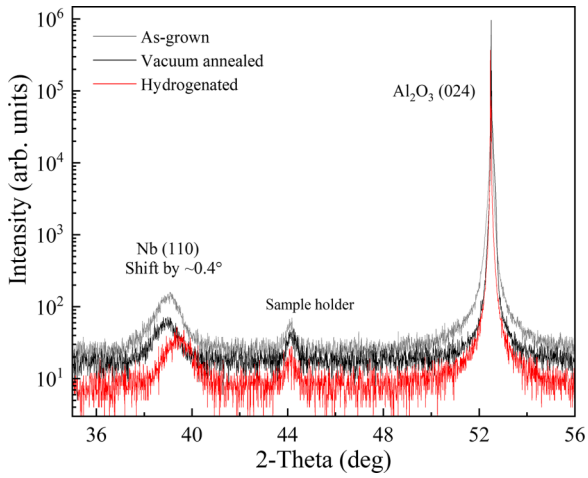

FIG. 3. X-ray diffraction of the Nb/Pd bilayer grown on *r*-cut sapphire substrate before and after RTH process at 300°C.

where $d_{(110,BH)}$ and $d_{(110,\ AH)}$ are interplanar spacing of sample before and after hydrogenation, respectively. The out of plane contraction occurs upon the RTH process, with an estimated stress of ~ 700 MPa equivalent to an $\sim 9\%$ intrinsic stress.

Furthermore, the Nb (101) peak position increases by $\sim 0.13^\circ$ to 38.48°, similarly to the Nb (110) (Fig. 2). The Nb (200) and Nb (211) peaks both shift to a higher angle by $\sim 0.1^\circ$ and $\sim 0.2^\circ$, respectively, whereas the Nb (310) peak shows no significant change. This implies that the RTH process produces both an in-plane and out of plane contraction. The Poisson's ratio of the thin film is calculated to be 0.29 after the RTH process, which indicates a hydrogen embrittlement [39]. The x-ray pole figure analysis displays a highly twinned microstructure that leads to sixfold symmetry in the Nb lattice, as shown in Supplemental Fig. S8 and Table S2 in the Supplemental Material [40].

In addition, nonuniform strain and grain size are analyzed using the Williamson-Hall method [41] shown in Supplemental Table S1 and Fig. S2 [40]. The as-grown sample has a positive strain and a grain size of ~ 26 nm. After the RTH process, the peak width distribution is nonlinear. As a result, the strain and grain size cannot be extracted accurately. This might be related to the Nb thin film having a network of grain boundaries that contains oxygen [42].

Figure 3 displays x-ray diffraction of the Nb/Pd bilayer grown on *r*-cut sapphire substrate before and after the RTH process at 300°C. The measurement is only done in the specular geometry. The vacuum annealed sample is added to understand the effect from temperature. The Nb/Pd bilayer grown on the *r*-cut sapphire substrate exhibits (110) texture, which is similar to the film grown on the *c*-cut sapphire substrate.

It is found that the Nb (110) peak shifts to a higher angle by $\sim 0.5^\circ$, after the RTH process in which the hydrogen-induced compressive stress is estimated to be as high as ~ 1.83 GPa accommodating more than 25% of intrinsic stress. In addition, opposite to the samples grown on *c*-cut substrates, the peak width in the samples grown on *r*-cut substrates shows no significant change with or without hydrogen loading.

TABLE I. X-ray reflectivity parameters extracted from the fitting of Nb/Pd bilayers x-ray spectra. The labels "V," "H," and "AG" stand for vacuum annealing, RTH, and as-grown sample, respectively, and the number after the label indicates the process temperature. Density of the Nb film is taken as 8.4 g/cm^3. These fits have an overall $\log R_1 < 0.005$ which indicates a good fit.

Label	Thickness (nm)	Roughness (nm)	Scattering factor (*e*/atom)
	Nb grown on *c*-cut substrate		
AG	101.2	1.7	41.0
V150	96.3	1.9	39.6
V200	96.1	2.0	38.7
V250	97.7	1.9	40.2
V300	98.5	2.0	40.1
H150	100.3	1.4	40.3
H200	100.2	1.7	38.6
H250	100.9	2.8	42.3
H300	101.6	2.1	40.1
	Nb grown on *r*-cut substrate		
AG	101.6	1.3	41.8
V200	100.8	1.2	42.3
V250	101.1	1.1	42.8
V300	102.4	1.5	43.5
V350	101.9	1.2	43.9
H200	98.8	2.8	41.4
H250	99.5	2.7	42.3
H300	99.4	2.1	40.6
H350	102.1	1.6	43.2

Table I summarizes the x-ray reflectivity fitting of the Nb/Pd bilayers grown on *c*-cut and *r*-cut sapphire substrates. For the sample grown on a *c*-cut substrate, vacuum annealing reduces the thickness of the film which hints at the relief of growth stress and improvement of crystallites [43]. In the RTH processed sample, the thickness is slightly lower than the as-grown sample but much higher than the vacuum annealed sample. Hence, the sample retains similar surface properties after hydrogenation, and the effect from annealing temperature is small.

In the *r*-cut sample, vacuum annealing and as-grown samples exhibit similar surface properties, while the RTH processed sample shows an increase of surface roughness along with the reduction of thickness. This should be related to the hydride formation [26]. The "H350" sample is an exception that shows nearly the same surface properties as the "V350." This implies that the hydride formation might be hindered due to the instability of hydride at higher temperature [12].

The superconducting transition temperatures are obtained from the ZFC branch of magnetization measurements. We determine the transition temperature from the separation point of magnetization between ZFC and FC branches, where the magnetization reaches its background value at higher temperatures (see Supplemental Fig. S3) [40]. The as-grown Nb sample $T_c = 8.78$ K. Given that the bulk Nb has a T_c of 9.2 K, the impurity level is estimated to be less than 0.5% [28]. Figure 4 shows measurements from a few selected samples highlighting the effect of RTH temperature for samples grown on different substrates. Figure 4(a) compares *r*-cut (red triangles) and *c*-cut (blue squares) samples hydrogenated at

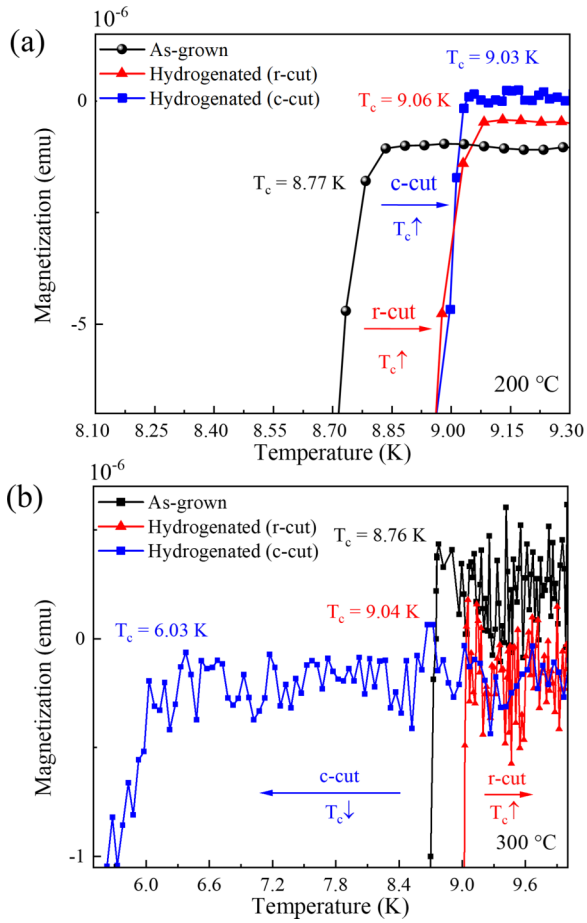

FIG. 4. Magnetization measurements of Nb/Pd bilayer before and after hydrogenation. (a) Comparison of critical temperature for the as-grown *c*-cut, *c*-cut, and *r*-cut samples hydrogenated at 200°C. (b) Comparison of critical temperature for the as-grown *r*-cut, *r*-cut, and *c*-cut samples hydrogenated at 300°C.

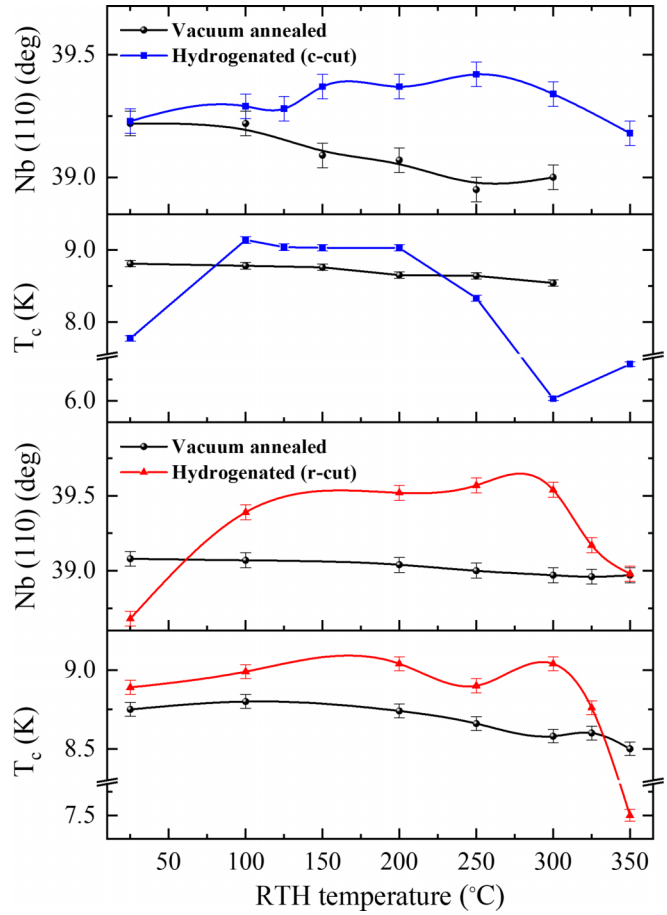

FIG. 5. Summary of the position of Nb (110) peak and T_c for the samples grown on *c*-cut and *r*-cut sapphire substrates as a function of RTH temperatures. The same hydrogenation process and pressure were used for all samples.

200°C with the as-grown (black circles) sample. After hydrogenation at 200°C, the T_c increases by $\sim 3.2\%$ in both *c*-cut and *r*-cut samples. The highest T_c observed here is ~ 9.06 K, with a decrease in superconducting volume fraction in the very same sample (see Supplemental Fig. S3) [40]. To compare the effect of RTH temperature, similar measurements are shown for *r*-cut and *c*-cut samples annealed at 300°C in Fig. 4(b). Applying the same RTH protocol at 300°C results in an increase by $\sim 2.7\%$ for the *r*-cut sample, while the *c*-cut sample surprisingly shows a significant decrease.

Figure 5 summarizes the x-ray Nb (110) peak position and T_c as a function of RTH temperature for *c*-cut (blue) and *r*-cut (red) samples. In the samples grown on *c*-cut substrates, the T_c increases when the hydrogenation temperature is at or below 200°C except for the one at room temperature, followed by the Nb (110) peak moving to a higher angle. The maximum compressive stress is estimated to be ~ 0.8 GPa. When the hydrogenation temperature is above 200°C, the T_c starts to decrease, but the Nb (110) peak still remains at a higher angle until 350°C. In the samples grown on *r*-cut substrates, the T_c increases when the hydrogenation temperature is below 350°C, and a lattice contraction always occurs. At above 325°C, the T_c begins to decrease with a lattice expansion and falls below the detection limit at 375°C.

IV. DISCUSSION

The evolution of the T_c of Nb films during rapid thermal hydrogenation arises from the following considerations. Initially, the formation of Nb (110) on *c*-cut and *r*-cut oriented sapphire substrates is known to generate strong lattice mismatch [33,34], resulting in high intrinsic stress and less epitaxial constraint. During the deposition, as the thickness of Nb increases, stress will accumulate until it exceeds the yield point of the film [38], leading to plastic strain, which leads to formation of misfit dislocations between the film and substrate to accommodate the lattice mismatch. This can explain the differences observed in the XRD spectra (Figs. 2 and 3) of the as-grown samples, where the Nb film grown on *r*-cut sapphire has a broader and less intense diffraction peak compared to the film on *c*-cut sapphire.

During the first stage of RTH, the sample is suddenly exposed to a high temperature and starts warming up. This leads to an extrinsic thermal stress σ_T, which can be described

as [44]

$$\sigma_T \propto (T_{\text{dep}} - T_{\text{hyd}})\Delta\alpha - \varepsilon^{\text{pl}}. \quad (4)$$

Here, $\Delta\alpha$ is the difference between the thermal expansion coefficient of niobium and sapphire, T_{dep} is the deposition temperature used for the growth of Nb films, T_{hyd} is the RTH temperature, and ε^{pl} is the plastic strain at the annealing temperature assumed to be constant. Since the thermal expansion coefficient of Nb is about 36% larger than sapphire [45,46], a steady compressive stress is generated as the sample warms up.

Simultaneously, before the thermal stress can be relaxed through any plastic strain, a large amount of hydrogen gas is introduced rapidly into the system. Those misfit dislocations formed during the deposition of Nb films become potential nucleation sites for the hydrides [26]. Due to the high intrinsic stress within the film, phase transformation is severely hindered [47], and hydride domains will be limited, and some might not even grow after nucleation. In this fashion, the entire thin film is supposed to have a much lower hydrogen concentration. According to the Nb-H phase diagram [12], at ~ 0.3 MPa of pressure, we expect to produce a hydride nucleus in the stoichiometric form NbH_x: $0.9 \leqslant x \leqslant 2$ at different temperatures. At this stoichiometry, the hydride phase was previously reported to exhibit an out of plane expansion along the [111] direction and an in-plane contraction along the [002] direction [48]. The in-plane contraction due to the formation of hydrides likely mediates the compressive stress from thermal expansion. As a result, when the temperature and pressure are stabilized, the system soon reaches an equilibrium state, in which the thermal stress is mostly released by the nucleation of hydrides, while the intrinsic stress is dominant and prevents further hydride growth.

In the final stage, the sample is removed and rapidly cooled. Thermal contraction is supposed to lead to tensile stress in the Nb film, which generates strain in the in-plane direction to elongate the film to match with the substrate, and strain in the out of plane direction to shrink the film to compensate for the in-plane elongation. However, there is limited epitaxial constraint between the Nb film and substrate, due to the specific growth condition used [49]. As a result, the thermal contraction is dominant and shrinks the Nb film both in-plane and out of plane as has been seen in the x-ray diffraction (Fig. 2). If the compressive stress is too high and exceeds the Nb yield, microcracks are expected to occur within the film [38], which might be responsible for the increase of surface roughness after hydrogenation (Table I). Furthermore, the c-cut and r-cut samples have different intrinsic stresses, where the distribution and amount of misfit dislocations are supposed to differ. As a result, thermal stress relaxes differently and produces additional final stress.

As for the superconductivity, the T_c increases due to the mechanical stress applied to the Nb film. This can be indirectly proved by the gas desorption experiment shown in Supplemental Figs. S5–S7 [40], where the T_c decreases from 9.06 K (before desorption) to 8.90 K (after desorption), and the Nb (110) x-ray peak shifts, from 39.24° (before desorption) to 39.11° (after desorption). Theoretically, increasing the T_c to about 9.06 K in Nb requires a static pressure corresponding to 2.3 GPa [50]. The previous result is similar to our experimental findings, where increased out of plane stress after the RTH process is calculated to be ~ 1.83 GPa (Fig. 3). On the other hand, the T_c increase may also be affected by the removal of impurities in the Nb film. Impurities could potentially be the nucleation sites of hydrides, where they are enclosed by hydride nuclei and isolated from the rest of the film. Given that the T_c of pure Nb is 9.2 K, approximately 67% of the impurities must be removed through the RTH procedure, to decrease the impurity level to less than 0.15%.

In summary, the reduction of superconductivity in films grown on c-cut sapphire can be explained by an enhancement of the hydrogen diffusion within its structure. The highly ordered crystal structure enhances the diffusion of H atoms and favors the formation of hydrides at room temperature. However, at higher temperatures ($100°C \leqslant T \leqslant 200°C$), hydride formation is limited due to the instability of the hydride phase. The remaining hydrides do not significantly impact the superconductivity; instead they generate an internal stress as high as a few GPa within the film. At high temperatures ($\geqslant 250°C$), the strain has saturated, which leads to the stress relaxation, resulting in a loss of internal stress which favors the hydride formation.

For films grown on r-cut sapphire, at room temperature, hydrogen diffusion is restricted due to the extremely small grain size [51]. The oxygen impurities between crystal grains might be removed by hydrogen infiltration [40], resulting in an increase of superconductivity. At elevated temperatures ($100°C \leqslant T \leqslant 300°C$), hydride formation is limited and internal stress begins to dominate in the Nb film, which is similar to the c-cut sample at higher temperature. Above 350°C, presumably the recrystallization process of the Nb film enhances the formation of hydrides which suppresses the superconductivity.

V. CONCLUSION

We have successfully manipulated the superconducting transition temperature of Nb/Pd bilayer films through rapid thermal hydrogenation. We found that the T_c is a function of RTH temperature and can be modulated differently on c-cut and r-cut oriented substrates. The XRD and VSM measurements showed that both in-plane and out of plane Nb peaks shifted to higher angles after the RTH process along with a change of T_c, respectively. The x-ray analysis revealed an increase in surface roughness upon hydrogenation. We confirmed that results are reproducible on different sets of samples grown in the same batch through RTH. We propose a possible scenario to explain the evolution of the Nb film during each stage of the RTH process, which can perhaps rationalize hydrogen's role in improving the T_c of the Nb film. For a complete understanding of the microstructure and role of hydrogen in the Nb film, further experimental validations and modeling need to be combined. Operando spectroscopy of hydride domains in the Nb film during the RTH process such as conductive atomic force microscopy or micro-Raman spectroscopy could be used to investigate the fundamental growth mechanism of hydrides on the surface of the Nb film. Neutron reflectometry could be used to determine the hydrogen content and crystallographic properties.

These could be combined with a gas desorption experiment for possible identification of the location of the hydrogen in the Nb film. Moreover, there are still potential parameters to explore in the RTH process to make use of the stress in different material systems. Such techniques might help improve not only T_c but also the manufacturability of hydrogenated superconductors.

All the data in the study are available upon request to the corresponding author.

ACKNOWLEDGMENT

This research was supported by a grant from the National Science Foundation (DMR-2132389).

[1] N. W. Ashcroft, Metallic Hydrogen: A High-Temperature Superconductor? Phys. Rev. Lett. **21**, 1748 (1968).

[2] N. W. Ashcroft, Hydrogen Dominant Metallic Alloys: High Temperature Superconductors? Phys. Rev. Lett. **92**, 187002 (2004).

[3] D. Sun, V. S. Minkov, S. Mozaffari, Y. Sun, Y. Ma, S. Chariton, V. B. Prakapenka, M. I. Eremets, L. Balicas, and F. F. Balakirev, High-temperature superconductivity on the verge of a structural instability in lanthanum superhydride, Nat. Commun. **12**, 6863 (2021).

[4] X. Ye, N. Zarifi, E. Zurek, R. Hoffmann, and N. W. Ashcroft, High hydrides of scandium under pressure: Potential superconductors, J. Phys. Chem. C **122**, 6298 (2018).

[5] H. Liu, I. I. Naumov, R. Hoffmann, N. W. Ashcroft, and R. J. Hemley, Potential high- T_c superconducting lanthanum and yttrium hydrides at high pressure, Proc. Natl. Acad. Sci. USA **114**, 6990 (2017).

[6] A. P. Drozdov, P. P. Kong, V. S. Minkov, S. P. Besedin, M. A. Kuzovnikov, S. Mozaffari, L. Balicas, F. F. Balakirev, D. E. Graf, V. B. Prakapenka *et al.*, Superconductivity at 250 K in lanthanum hydride under high pressures, Nature (London) **569**, 528 (2019).

[7] E. Snider, N. Dasenbrock-Gammon, R. Mcbride, M. Debessai, H. P. Vindana, K. Vencatasamy, K. V. Lawler, A. Salamat, and R. P. Dias, Retraction Note: Room temperature superconductivity in a carbonaceous sulfur hydride, Nature (London) **610**, 804 (2022).

[8] J. E. Hirsch, Comment on "Room-temperature superconductivity in a carbonaceous sulfur hydride, by Elliot Snider *et al.*, Europhys. Lett. **137**, 36001 (2022).

[9] R. P. Gupta and S. K. Sinha, Superconductivity in metallic hydrogen, in *Superconductivity in d- and f-Band Metals, Second Rochester Conference*, edited by D. H. Douglass (Springer, Berlin, 1976), pp. 583–592.

[10] J. E. Hirsch and F. Marsiglio, Nonstandard superconductivity or no superconductivity in hydrides under high pressure, Phys. Rev. B **103**, 134505 (2021).

[11] H. M. Syed, C. J. Webb, and E. M. Gray, Hydrogen-modified superconductors: A review, Prog. Solid. State Chem. **44**, 20 (2016).

[12] J. J. Reilly and R. H. Wiswall, The higher hydrides of vanadium and niobium, Inorg. Chem. **9**, 1678 (1970).

[13] M. Strongin, M. El-Batanouny, and M. A. Pick, Structure of Pd overlayers on Nb and Ta and the relationship to hydrogen uptake, Phys. Rev. B **22**, 3126 (1980).

[14] M. Lagos and I. K. Schuller, Enhancement of hydrogen uptake in metals and subsurface bonding, Surf. Sci. Lett. **138**, L161 (1984).

[15] M. Lagos, G. Martinez, and I. K. Schuller, Kinetics of hydrogen absorption in transition metals and subsurface bonding, Phys. Rev. B **29**, 5979(R) (1984).

[16] A. H. Romero, I. K. Schuller, and R. Ramirez, Subsurface bonding of hydrogen in niobium: A molecular-dynamics study, Phys. Rev. B **58**, 15904 (1998).

[17] A. P. Durajski, Phonon-mediated superconductivity in compressed NbH_4 compound, Eur. Phys. J. B **87**, 210 (2014).

[18] G. Gao, R. Hoffmann, N. W. Ashcroft, H. Liu, A. Bergara, and Y. Ma, Theoretical study of the ground-state structures and properties of niobium hydrides under pressure, Phys. Rev. B **88**, 184104 (2013).

[19] J. M. Welter and F. J. Johnen, Superconducting transition temperature and low temperature resistivity in the niobium-hydrogen system, Z. Phys. B **27**, 227 (1977).

[20] M. Gupta, Why does hydrogen destroy superconductivity in niobium and lanthanum? Solid State Commun. **50**, 439 (1984).

[21] M. W. Ruckman, G. Reisfeld, N. M. Jisrawi, M. Weinert, M. Strongin, H. Wiesmann, M. Croft, A. Sahiner, D. Sills, and P. Ansari, XANES study of hydrogen incorporation in a Pd-Capped Nb thin film, Phys. Rev. B **57**, 3881 (1998).

[22] N. M. Jisrawi, M. W. Ruckman, T. R. Thurston, G. Reisfeld, M. Weinert, M. Strongin, and M. Gurvitch, Reversible depression in the T_c of thin Nb films due to enhanced hydrogen adsorption, Phys. Rev. B **58**, 6585 (1998).

[23] P. Klose, V. Roddatis, and A. Pundt, Tuning the stress state in Nb-thin films by lateral size confinement, Acta Mater. **222**, 117454 (2022).

[24] J. Lee, Z. Sung, A. A. Murthy, M. J. Reagor, A. Grassellino, and A. Romanenko, Discovery of Nb Hydride Precipitates in Superconducting Qubits, Fermi National Accelerator Lab Report NO. FERMILAB-PUB-21-676-SQMS-TD, 2021.

[25] F. Barkov, A. Romanenko, Y. Trenikhina, and A. Grassellino, Precipitation of hydrides in high purity niobium after different treatments, J. Appl. Phys. **114**, 164904 (2013).

[26] K. Nörthemann and A. Pundt, Double-locked nucleation and growth kinetics in Nb-H thin films, Phys. Rev. B **83**, 155420 (2011).

[27] S. Isagawa, Hydrogen absorption and its effect on low-temperature electric properties of niobium, J. Appl. Phys. **51**, 4460 (1980).

[28] G. Reisfeld, N. M. Jisrawi, M. W. Ruckman, and M. Strongin, Hydrogen absorption by thin Pd/Nb films deposited on glass, Phys. Rev. B **53**, 4974 (1996).

[29] R. Gunawan, M. Y. L. Jung, E. G. Seebauer, and R. D. Braatz, Optimal control of rapid thermal annealing in a semiconductor process, J. Process Control **14**, 423 (2004).

[30] A. Fiory, Recent developments in rapid thermal processing, J. Electron. Mater. **31**, 981 (2002).

[31] M. H. Lee, Y. Kalcheim, J. Del Valle, and I. K. Schuller, Controlling metal-insulator transitions in vanadium oxide thin films by modifying oxygen stoichiometry, ACS Appl. Mater. Interfaces **13**, 887 (2021).

[32] A. Glavic and M. Björck, GENX 3: The latest generation of an established tool, J. Appl. Cryst. **55**, 1063 (2022).

[33] A. R. Wildes, J. Mayer, and K. Theis-Brohl, The growth and structure of epitaxial niobium on sapphire, Thin Solid Films **401**, 7 (2001).

[34] T. Wagner, M. Lorenz, and M. Rühle, Thermal stability of Nb thin films on sapphire, J. Mater. Res. **11**, 1255 (1996).

[35] M. Dryś, J. Sosnowski, and L. Folcik, Phase equilibria in the niobium-gallium-iron system at 1000 °C, J. Less-Common Met. **68**, 175 (1979).

[36] R. Lakes and K. W. Wojciechowski, Negative compressibility, negative poisson's ratio, and stability, Phys. Status Solidi B **245**, 545 (2008).

[37] R. B. Ross, *Metallic Materials Specification Handbook* (Springer Science & Business Media, Berlin, 2013), pp. 264–265.

[38] M. Hamm, V. Burlaka, S. Wagner, and A. Pundt, Achieving reversibility of ultra-high mechanical stress by hydrogen loading of thin films, Appl. Phys. Lett. **106**, 243108 (2015).

[39] P. Cotterill, The hydrogen embrittlement of metals, Prog. Mater. Sci. **9**, 205 (1961).

[40] See Supplemental Material at http://link.aps.org/supplemental/10.1103/PhysRevB.xx.xxxxxx for the details of performed measurements and results, C. P. Bean, Magnetization of Hard Superconductors, Phys. Rev. Lett. **8**, 250 (1962).

[41] J. Pelleg, E. Elish, and D. Mogilyanski, Evaluation of average domain size and microstrain in a silicide film by the Williamson-Hall method, Metall. Mater. Trans. **36**, 3187 (2005).

[42] M. Murakami and T. Yogi, Strain in evaporated Nb thin films, J. Appl. Phys. **57**, 211 (1985).

[43] Y. W. Kim, S. G. Lee, and J. H. Choi, *Ex situ* annealing effect on Nb thin films prepared by dc magnetron sputtering, Phys. C: Supercond. **471**, 1193 (2011).

[44] B. R. York, Residual stress/strain analysis in thin films by x-ray diffraction, Crit. Rev. Solid State Mater. Sci. **20**, 125 (1995).

[45] G. K. White, M. L. Minges, R. B. Castanet, S. J. Collocott, P. D. Desai, C. Y. Ho, J. G. Hust, R. B. Roberts, and C. A. Swenson, Thermophysical properties of some key solids: An update, Int. J. Thermophys. **18**, 1269 (1997).

[46] K. Wang and R. R. Reeber, The role of defects on thermophysical properties: Thermal expansion of V, Nb, Ta, Mo and W, Mater. Sci. Eng., R **23**, 101 (1998).

[47] V. Burlaka, S. Wagner, M. Hamm, and A. Pundt, Suppression of phase transformation in Nb-H thin films below switchover thickness, Nano Lett. **16**, 6207 (2016).

[48] P. F. Miceli, H. Zabel, J. A. Dura, and C. P. Flynn, Anomalous lattice expansion of metal-hydrogen thin films, J. Mater. Res. **6**, 964 (1991).

[49] V. Oderno, C. Dufour, K. Dumesnil, A. Mougin, P. H. Mangin, and G. Marchal, Hexagonal surface structure during the first stages of niobium growth on sapphire (1120), Philos. Mag. Lett. **78**, 419 (1998).

[50] G. Pristáš, S. Gabáni, M. Orendáč, V. Komanický, and E. Gažo, Study of niobium thin films under pressure, Acta Phys. Pol. **126**, 1 (2014).

[51] T. O. Ogurtani, The kinetics of diffusion of hydrogen in niobium, Metall. Mater. Trans. B **2**, 3035 (1971).